Erschienen in: Oncogene ; 34 (2015), 32. - S. 4270-4277

The human oncoprotein and chromatin architectural factor DEK counteracts DNA replication stress

A Deutzmann[1,3], M Ganz[1], F Schönenberger[1], J Vervoorts[2], F Kappes[2] and E Ferrando-May[1]

DNA replication stress is a major source of DNA strand breaks and genomic instability, and a hallmark of precancerous lesions. In these hyperproliferative tissues, activation of the DNA damage response results in apoptosis or senescence preventing or delaying their development to full malignancy. In cells, in which this antitumor barrier is disabled by mutations (for example, in p53), viability and further uncontrolled proliferation depend on factors that help to cope with replication-associated DNA damage. Replication problems preferentially arise in chromatin regions harboring complex DNA structures. DEK is a unique chromatin architectural factor which binds to non-B-form DNA structures, such as cruciform DNA or four-way junctions. It regulates DNA topology and chromatin organization, and is essential for the maintenance of heterochromatin integrity. Since its isolation as part of an oncogenic fusion in a subtype of AML, DEK has been consistently associated with tumor progression and chemoresistance. How DEK promotes cancer, however, is poorly understood. Here we show that DEK facilitates cellular proliferation under conditions of DNA replication stress by promoting replication fork progression. DEK also protects from the transmission of DNA damage to the daughter cell generation. We propose that DEK counteracts replication stress and ensures proliferative advantage by resolving problematic DNA and/or chromatin structures at the replication fork.

INTRODUCTION

DEK is a biochemically and structurally unique non-histone chromatin protein which is conserved in all higher eukaryotes. It binds to non-B-form DNA structures, such as cruciform DNA or four-way junctions, regulates DNA topology and chromatin organization, and is essential for the maintenance of heterochromatin integrity.[1,2] At the cellular level, it displays pleiotropic functions and has been shown to influence differentiation, apoptosis, senescence and maintenance of cell stemness.[3–6] Since its isolation as part of an oncogenic fusion in a subtype of acute myeloid leukemia,[7] DEK has been consistently associated with tumor progression and chemoresistance.[8–10] Several lines of evidence, such as DEK-dependent formation of papilloma in a mouse model of skin cancerogenesis,[10] have led to its classification as a bona fide oncogene. In melanomas, high levels of DEK expression correlate positively with metastatic potential, chemoresistance and poor treatment outcome. Significantly, DEK expression levels can distinguish benign nevi from malignant melanoma, raising the possibility of using DEK as a tumor marker.[8,9]

We and others have shown that DEK is involved in DNA repair and the response to DNA damage: cells with downregulated DEK expression are hypersensitive to genotoxic insults and show increased susceptibility to sublethal doses of DNA damaging agents.[11,12] DNA repair is affected by DEK ablation, as DNA strand breaks (DSBs) are repaired less efficiently and nonhomologous end-joining appears to be defective.[12,13] DEK is also a substrate for covalent and non-covalent poly(ADP-ribosyl)ation (PARylation),[12,14] a posttranslational modification known to modulate DNA repair. So far, data suggest that DEK may act as a factor protecting from DNA damage and sustaining DNA repair, in line with the poor response to chemotherapy seen in DEK-overexpressing tumors. However, cancer development is most often characterized by defective DNA repair and genomic instability[15] questioning a role of DEK as a genuine oncogenic factor.

This apparent conundrum prompted us to elucidate the link between the tumorigenic properties of DEK and its role in the response to DNA damage. We hypothesized that DEK might be implicated in the handling of DNA damage arising during DNA replication. Our assumption was based on the following previous evidence: (i) DEK impacts on DNA replication *in vitro*,[16] (ii) it binds preferentially to cruciform DNA and four-way junctions, structures that may arise at stalled forks[17] and (iii) its expression levels correlate positively with proliferative potential.[18]

According to the oncogene-induced DNA damage model for tumor development,[19,20] the ability to tolerate high levels of replication stress is a distinguishing feature of advanced cancers. In these cells, in which the DNA damage response induced by replication-associated DNA damage has been circumvented by mutations in checkpoint regulators, tumor suppressors or DNA repair genes, factors that help to cope with replication-associated DNA damage, may support cancer 'fitness' as recently proposed for ATR and CHK1.[21,22]

Here we show that DEK impacts positively on replication fork progression, in particular under conditions of DNA replication stress, and that it attenuates the consequences of replication-born DNA damage in mitosis and daughter cells. On the basis of these

[1]Bioimaging Center, Department of Biology, University of Konstanz, Konstanz, Germany and [2]Institute of Biochemistry and Molecular Biology, Medical School, RWTH Aachen University, Aachen, Germany. Correspondence: Professor E Ferrando May, Bioimaging Center, Department of Biology, University of Konstanz, PO Box 604, Universitätsstrasse 10, D 78464 Konstanz, Germany.
E mail: elisa.may@uni konstanz.de
[3]Current address: Division of Oncology, Center for Clinical Sciences Research, Stanford University School of Medicine, Stanford, CA, USA.

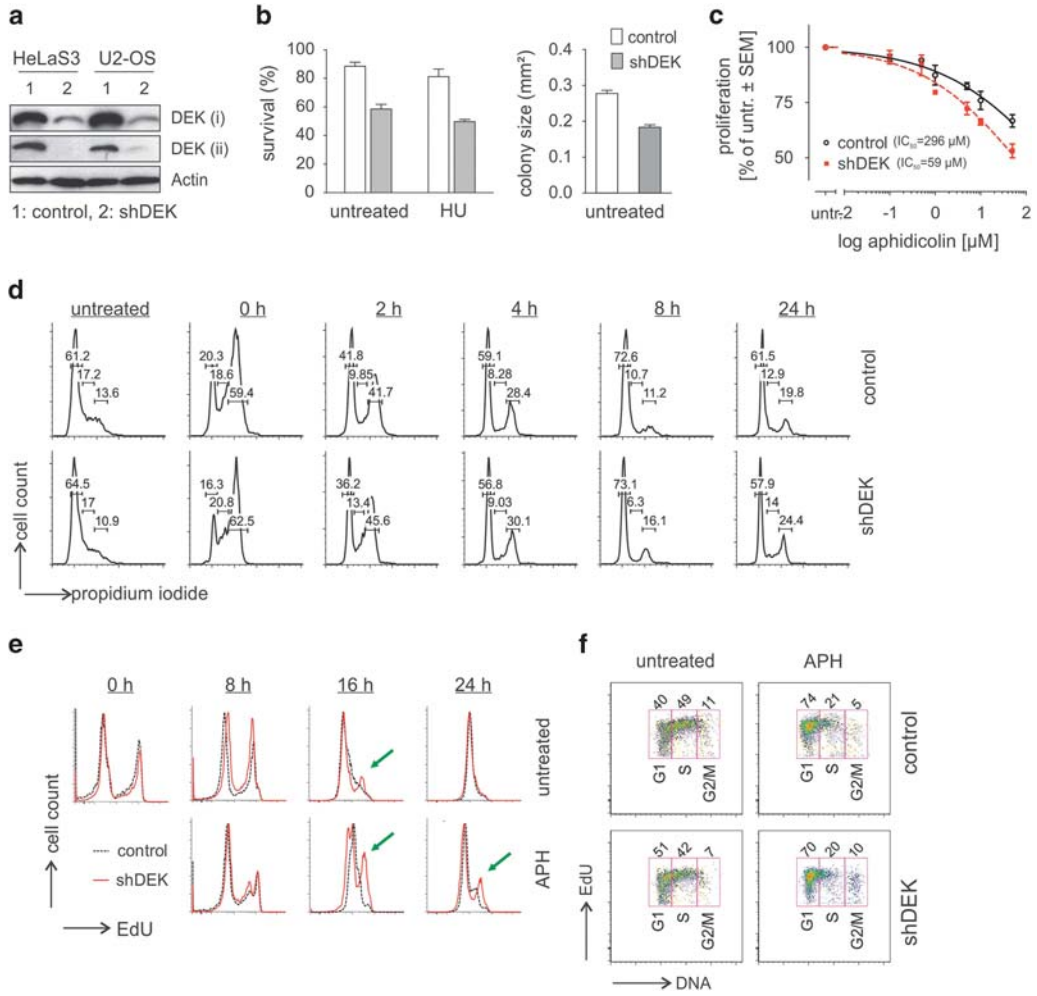

Figure 1. Loss of DEK results in cell cycle delay and reduced proliferation. (**a**) Western blot analysis of DEK expression in HeLa S3[12] and U2-OS cells following shRNA-mediated downregulation. U2-OS control and shDEK cells were generated by transduction with lentiviral particles delivering either DNA coding for a scrambled control shRNA (pLKO.1-scrambled shRNA, Sigma Mission) or a DEK-specific shRNA (pLKO.1-shDEK1165, Sigma Mission). For generation of lentiviral particles, the packaging cell line Hek293FT was transfected with pMD2.G, psPAX2 and pLKO.1. Infected U2-OS cells were selected with 2 µg/ml puromycin (Calbiochem, Merck Millipore, Darmstadt, Germany) and kept as pools. DEK was specifically visualized using (i) rabbit anti-DEK (1:20 000; K 877 (ref. 12)) and (ii) mouse anti-human DEK (1:500, BD Transduction Laboratories, BD Biosciences, San Jose, CA, USA). Actin served as loading control and was labeled using mouse anti-actin (1:50 000, clone C4, Chemicon, Merck Millipore). Secondary antibodies were HRP-labeled goat-anti-mouse or -anti-rabbit IgG (both from Dako, Hamburg, Germany). (**b**) Clonogenic survival assay. HeLa S3 control and shDEK cells[12] were either treated with 1 mM HU (Sigma-Aldrich, St Louis, MO, USA) for 24 h before seeding or left untreated. Colonies were fixed and stained with 6% glutaraldehyde, 0.5% crystal violet (Sigma-Aldrich), counted and the colony size was determined after 7 days using ImageJ. Error bars represent s.e.m. The experiment was run in triplicates. The effect of DEK depletion on plating efficency was confirmed additionally in U2-OS cells in two independent experiments (data not shown). (**c**) Proliferation assay. HeLa S3 control and shDEK cells were treated with increasing concentrations of APH (Sigma-Aldrich) for 24 h. Proliferation was assessed by fluorimetric Alamar Blue assay (Invitrogen, Life Technologies, Darmstadt, Germany) and normalized to the corresponding untreated sample. Data points represent the mean of three independent experiments. Error bars indicate s.e.m. (**d**) Flow cytometry analysis of cell cycle progression after synchronization in mitosis. Cells were seeded one day before treatment with 100 ng/ml nocodazole for 14 h. Cells were released from nocodazole by washing three times with warm phosphate-buffered saline and were grown in full medium for indicated time periods. After that, cells were collected in 500 µl phosphate buffered saline (PBS) and fixed in 4.5 ml − 20 °C cold 80% ethanol for at least 2 h. A treatment with RNase (200 µg/ml DNAse-free RNase, 10 mM Tris HCl, 1 mM EDTA, pH 7.8) was performed for 2 h at 37 °C before cells were stained with propidium iodide (100 µg/ml propidium iodide, 10 mM Tris HCl, 1 mM EDTA, pH 7.8) for 30 min. Flow cytometry analysis was performed using a FACS Calibur (BD Biosciences). Data were processed and analyzed with FlowJo (Tree Star Inc., USA). (**e**) Flow cytometry analysis of cell cycle progression after pulse-labeling with EdU. HeLa S3 control and shDEK cells were labeled with EdU (10 µM, Invitrogen) for 1 h and were either left untreated (left panels) or treated with APH (right panels, 200 nM, Sigma-Aldrich) for the indicated time periods. Cells were fixed with 4% paraformaldehyde (Sigma-Aldrich). EdU- labeled cells were detected using the Click-IT EdU Assay (Invitrogen) with Alexa 488-azide as detection reagent. Histograms show Alexa 488-specific signal intensity. Flow cytometry analysis was done using a FACS Aria (BD Biosciences). The experiment was performed in duplicate with similar results. At the time point 0 h, S phase, EdU-positive cells are represented by the left peak, whereas unlabeled cells give rise to the peak on the right. As the cellular EdU levels decrease due to duplication of DNA and cell division, the two peaks merge into one of intermediate intensity. In APH-treated cells, this process is delayed, more evidently if DEK expression is downregulated (green arrows). (**f**) Flow cytometry analysis of cell cycle distribution 24 h after Edu pulse-labeling. U2-OS control and shDEK cells were pulse-labeled with EdU (10 µM, Invitrogen) for 30 min and were either left untreated or treated with APH (200 nM, Sigma-Aldrich) for 24 h. Cells were fixed in 4% paraformaldehyde (Sigma-Aldrich). Before flow cytometry analysis using an LSR Fortessa (BD Biosciences), EdU was labeled as described in **e** using the Click-IT EdU Assay (Invitrogen) employing Alexa Fluor-488-azide. Cells were treated with RNase for 2 h at 37 °C and DNA was stained with Hoechst 33342 (Invitrogen). The graph shows the distribution of the EdU-positive subpopulation 24 h after labeling. Under APH treatment, twice as many shDEK cells reside in G2/M as compared with control (10% vs 5%).

data, we propose that DEK contributes to resolve problematic DNA and/or chromatin structures at the replication fork via its known function as chromatin architectural factor. Hence, high levels of DEK expression may provide proliferative advantage crucial for cancer development and maintenance.

RESULTS AND DISCUSSION

DEK promotes proliferation and fork progression under replication stress

To explore the hypothesis that the pro-oncogenic properties of DEK might be linked to a role of this protein in DNA replication, we first investigated how DEK affects survival and cell proliferation under replication stress induced by replication inhibitors hydroxyurea (HU) and aphidicolin (APH) in control HeLa S3 and DEK knockdown cells (shDEK, Figure 1a). HU was employed at a concentration of 1 mM, at which it immediately stalls the replication fork.[23] APH, a reversible inhibitor of DNA polymerases,[24] was used at nanomolar concentrations known to slow down fork progression but permit continuous replication.[25]

First, clonogenic survival assays were performed after HU treatment. Here, we observed that survival of shDEK cells as compared with control was reduced irrespective of treatment, which indicated an effect of DEK downregulation on plating efficiency, while treatment itself (HU, 24 h) had only a minor effect (compare second and fourth bar in Figure 1b, left panel). Colony size was significantly reduced in shDEK cells even in the absence of treatment, suggestive of impaired cell growth (Figure 1b, right panel). The effect of APH was assessed by Alamar Blue proliferation assay. shDEK cells were highly sensitive towards APH treatment and displayed a fivefold lower IC_{50} value for proliferation impairment by this drug than control cells (Figure 1c).

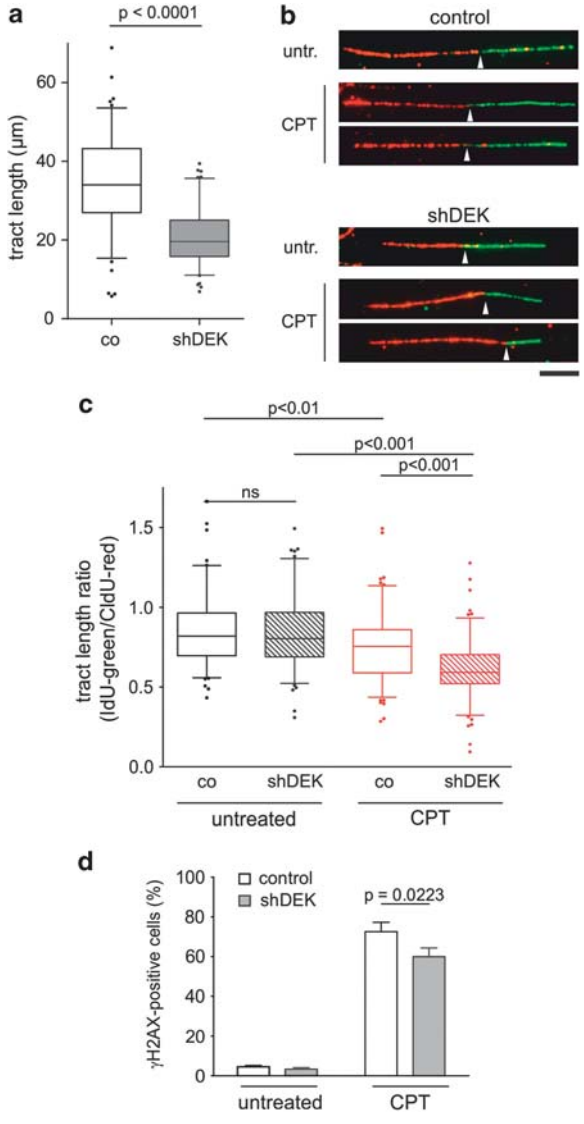

Figure 2. Replication fork progression is impaired in the absence of DEK. (**a**) DNA fiber analysis of cells with downregulated DEK expression. U2-OS control and shDEK cells were pulse-labeled successively with CldU (30 µM, Sigma-Aldrich) and IdU (250 µM, Sigma-Aldrich) for 20 min each. DNA fibers were labeled with anti-BrdU antibodies from Abcam (detects CldU) and anti-BrdU antibodies from Becton Dickinson (detects IdU), respectively, and visualized via epifluorescence microscopy. As secondary antibodies, anti-mouse Alexa 488 (Invitrogen) and anti-rat Cy3 (Jackson Immuno Research Laboratories, West Grove, PA, USA) were used. Image acquisition was done at a Zeiss Cellobserver HS equipped (Zeiss, Oberkochen, Germany) with an αPlan-Fluar ×100/1.45 Oil objective lens. Fiber tract lengths were determined using the 'Fibers' tool of a custom-built ImageJ macro ('BIC macro toolkit', available online: http://www.bioimaging-center.uni-konstanz.de/image-analysis/imagej-macro-toolkit/). At least 50 (CldU+IdU labeled) tracts per experimental condition were analyzed in two independent experiments with similar outcome. The graph shows the sum of these two experiments (>100 tracts per condition). Whiskers indicate 10th 90th percentile. Error bars represent s.e.m. Student's *t*-test was done using GraphPad Prism 5.02 (GraphPad Software). Data show a significant reduction in fiber tract length in cells with downregulated DEK expression. (**b**) Representative images of the experiments described in **a** and **c**. CldU tracts are stained in red, IdU tracts in green. White arrows indicate CldU/IdU transition. Scale bar, 5 µm. (**c**) DNA fiber analysis under replication stress conditions. U2-OS control and shDEK cells were first pulse-labeled with CldU as in **a** followed by labeling with IdU (250 µM) either alone (untreated), or in the presence of camptothecin (CPT; 25 nM, Sigma-Aldrich) for 20 min. The IdU-/CldU-tract length ratio is shown. At least 50 (CldU+IdU labeled) tracts per experimental condition were analyzed in two independent experiments with similar outcome. Graph shows the sum of these two experiments (>100 tracts per condition). Whiskers indicate 5th 95th percentile. Error bars represent s.e.m. One-way analysis of variance followed by Tukey's multiple comparison test was done using GraphPad Prism 5.02 (GraphPad Software). Impairment of replication fork progression by CPT is more pronounced in cells with downregulated DEK expression. (**d**) Quantification of γH2AX foci induced by camptothecin treatment. U2-OS control and shDEK cells were either left untreated or treated with 25 nM CPT for 1 h. S phase cells were labeled with EdU (10 µM, Invitrogen) for 30 min and EdU was visualized by labeling with Alexa-647-Azide (Click-IT EdU, Invitrogen). DNA damage was visualized with antibodies specific for γH2AX (anti-phospho H2AX (Ser139), 1:500, clone JBW301, Biomol, Hamburg, Germany). Goat anti-mouse Alexa Fluor-488 (Invitrogen) was used as secondary antibody. DNA was counterstained using Hoechst 33342 (Invitrogen). Image acquisition was performed at room temperature employing a laser scanning confocal microscope (LSM 510 Meta, Zeiss) equipped with a Plan Neofluar ×40/1.30 Oil DIC objective. Only S-phase cells identified by EdU labeling were evaluated. The percentage of γH2AX positive cells were counted using the 'Foci Counter' tool which is a part of the BIC macro toolkit (available online, see legend in **a**). At least 100 EdU-positive cells were evaluated per sample. Graph shows the mean with s.e.m. of three independent experiments. Student's *t*-test was done using GraphPad Prism 5.02 (GraphPad Software). In the presence of CPT, downregulation of DEK expression led to a decrease of the percentage of γH2AX-positive cells as compared with control cells.

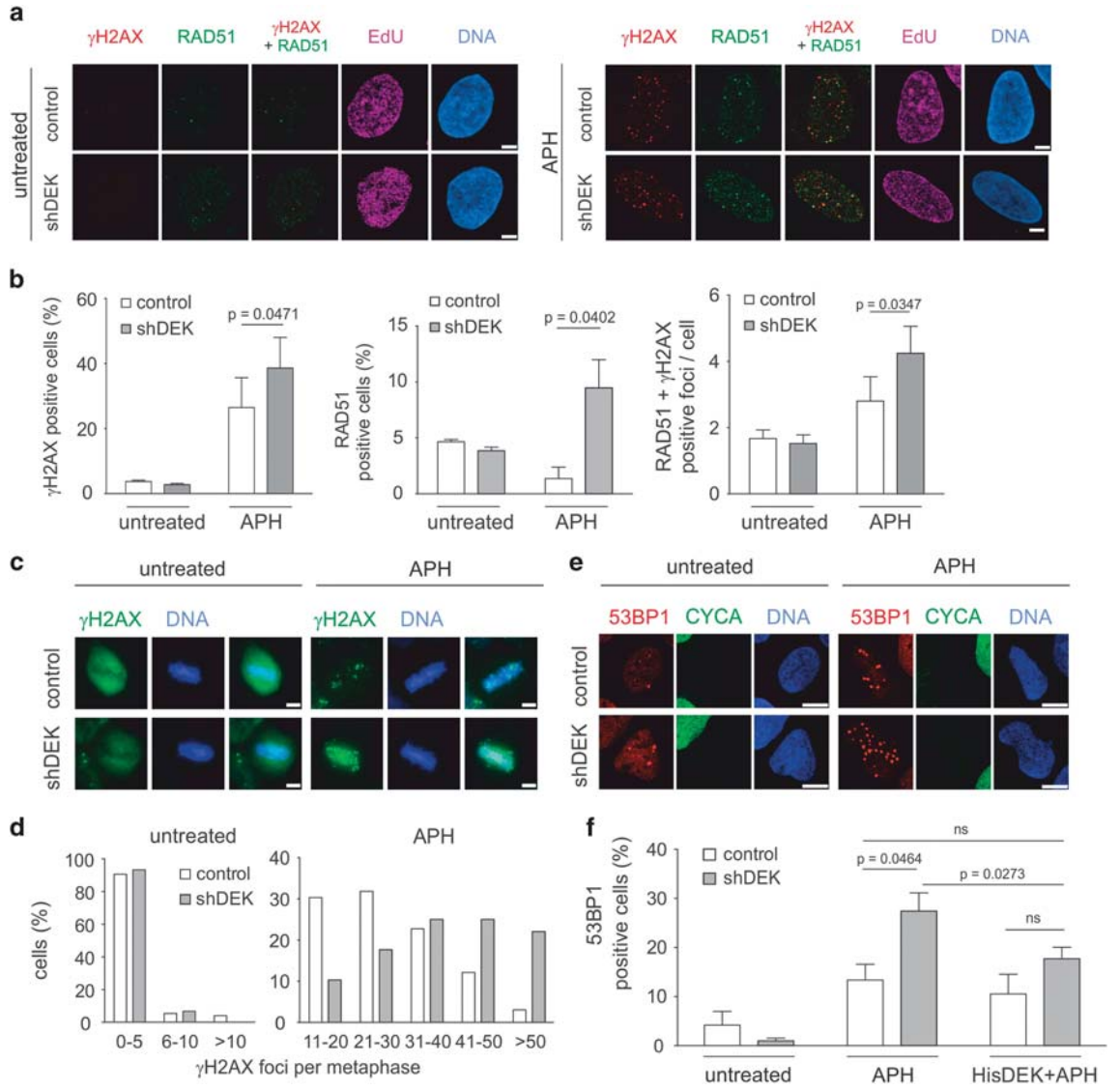

Figure 3. DEK limits the occurrence of stalled replication forks and protects daughter cells from replication-born DNA damage. (**a**) Exemplary confocal images of immunofluorescence analysis of nuclei of U2-OS cells in S phase. U2-OS control and shDEK cells were either left untreated (left panel) or treated with 200 nM APH for 24 h (right panel). Cells were labeled with EdU (10 μM, Invitrogen) for 30 min to visualize S phases, and with antibodies specific for γH2AX (anti-phospho H2AX (Ser139), 1:500, clone JBW301, Biomol) and RAD51 (rabbit anti-RAD51, 1:50, clone H-92, Santa Cruz Biotechnology, Dallas, TX, USA) as markers for stalled replication forks. EdU was visualized by labeling with Alexa-488-Azide (Click-IT EdU, Invitrogen). Goat anti-rabbit Alexa Fluor-546 and goat anti-mouse Alexa Fluor-647 (both from Invitrogen) were used as secondary antibodies. DNA was counterstained using Hoechst 33342 (Invitrogen). Image acquisition was performed at room temperature employing a laser scanning confocal microscope (LSM 510 Meta, Zeiss) equipped with a Plan Neofluar ×40/1.30 Oil DIC objective. Exemplary confocal images are shown. Scale bar, 5 μm. (**b**) Quantification of images as shown in **a**. Only S-phase cells identified by EdU labeling were evaluated. The percentage of γH2AX- and RAD51-positive cells, and the number of γH2AX/RAD51 double-positive foci were counted using the 'Foci Counter' tool, which is part of the BIC macro toolkit (available online, see legend to Figure 2a). At least 100 EdU-positive cells were evaluated per sample. Graph shows the mean with s.e.m. of three independent experiments performed as described in **a**. Student's *t*-test was done using GraphPad Prism 5.02 (GraphPad Software). In the presence of APH, downregulation of DEK expression led to an increase in the percentage of γH2AX-positive and RAD51-positive cells, as well as γH2AX/RAD51 double-positive foci as compared with control cells. (**c**) Downregulation of DEK leads to increased DNA damage at metaphase. U2-OS control and shDEK cells were either left untreated or treated with APH (200 nM, Sigma-Aldrich) for 24 h. Cells were labeled with γH2AX-specific antibodies (anti-phospho H2AX (Ser139), 1:500, clone JBW301, Biomol). Goat anti-mouse Alexa Fluor-488 or -564 (both from Invitrogen) were used as secondary antibodies. Metaphases were imaged by epifluorescence microscopy using a Zeiss Cellobserver HS equipped with a LD-Plan Neofluar ×40/0.60 objective. Exemplary z-projections are shown. Scale bar, 5 μm. (**d**) Quantification of γH2AX-positive foci on metaphase chromosomes. Data correspond to the sum of three independent experiments. At least 70 metaphases were evaluated per experimental condition. (**e**) Downregulation of DEK leads to increased formation of 53BP1 domains in G1 cells. U2-OS control and shDEK cells were either left untreated or treated with APH (200 nM) for 24 h. 53BP1 and CYCA were detected via specific antibodies (rabbit anti-53BP1, 1:200, clone H-300, Santa Cruz Biotechnology; mouse anti-cyclin A, 1:200, clone 6E6, Santa Cruz Biotechnology). Goat anti-rabbit Alexa Fluor-546 and goat anti-mouse Alexa Fluor-488 (both from Invitrogen) were used as secondary antibodies. Exemplary confocal images of untreated and APH-treated cells using a LSM 510 Meta (Zeiss) are shown. Scale bar, 5 μM. (**f**) 53BP1 nuclear bodies were quantified in CYCA-negative non-mitotic cells treated as in **e** and in control and shDEK cells supplemented with recombinant His-tagged DEK. Recombinant His-tagged DEK was added to a final concentration of 200 ng/ml 5 h before APH treatment and was present during APH treatment. Recombinant human full length His-DEK was purified via Ni-NTA resins from insect cells as described in Kappes *et al.*[12] Graph shows the mean with s.e.m. of three independent experiments. Student's *t*-test was done using GraphPad Prism 5.02 (GraphPad Software).

In further experiments, APH was used at a concentration of 200 nM which triggers replication stress but barely affected proliferation.

Having established that DEK positively affects cell growth in particular under mild replication stress in two independent experimental settings, we next investigated the influence of this protein on cell cycle progression. To this end we synchronized shDEK and control U2-OS cells in prometaphase of mitosis by nocodazole treatment and analyzed their cell cycle progression profiles via DNA histograms for up to 24 h after release from the nocodazole block (Figure 1d). At all time points analyzed, slightly more shDEK cells were in G2/M phase as compared with control cells. To explore this point in more detail, we pulse-labeled cells with 5-ethynyl-2′-deoxyuridine (EdU) in S phase and analyzed them for up to 24 h after release by flow cytometry (Figures 1e and f). Using this approach, we observed a persistance of the initial EdU-specific signal in shDEK cells (Figure 1e, green arrow), indicating that cell cycle progression is delayed. This effect was even more pronounced when cells were subjected to mild perturbance of replication using APH. We then analyzed this residual EdU-labeled population present after 24 h of exposure to APH by flow cytometry and observed an increase in the number of cells in G2/M phase when DEK was downregulated (10% EdU-positive shDEK cells as compared with 5% EdU-positive control cells in G2/M) corroborating the data from the nocodazole block (Figure 1d). These data are also in line with our previous work showing a G2/M arrest in HeLa cells with downregulated DEK expression.[1] Analysis of checkpoint markers by western Blot did not show a significant activation of ATM or the ATR downstream target CHK1, probably because of the very moderate levels of replication impairment elicited at the low APH concentration applied (Supplementary Figure 1). This type of mild chronic replication stress has been reported to remain undetected by cell cycle checkpoints thus becoming a serious threat to chromosomal integrity and genomic stability.[26] Altogether these data suggest that DEK promotes proliferation in particular under conditions of mild replication stress helping cells to overcome a cell cycle delay in G2/M and proceed to the next round of cell division.

To investigate a direct impact of DEK on DNA replication, as suggested by its influence on the response to the DNA polymerase inhibitor APH, we performed DNA fiber assays. First, we compared replication fork progression in untreated U2-OS control and shDEK cells by measuring fiber tract lengths. In untreated shDEK cells, both CldU- and IdU-labeled fiber tracts were significantly shorter as compared with control cells resulting in a reduced averaged total fiber tract length (20.7 ± 0.7 μm vs 34.5 ± 1.1 μm; Figures 2a and b). Thus, DEK downregulation alone slowed down replication fork velocity by about 30%, which is in accordance with the reduced proliferative potential of shDEK cells. Next, we perturbed DNA replication using a low dose of the topoisomerase 1 (TOP1) inhibitor camptothecin (CPT). This treatment has been shown to slow down the replication fork, and, importantly, also to induce replication fork reversal. The latter step is predicted to facilitate fork recovery and limit DSB formation.[27] CPT treatment reduced fork progression resulting in a decreased tract length ratio in both control and shDEK cells. Notably, this effect was much more pronounced when DEK expression was downregulated (Figures 2b and c), evincing a function of DEK at the replication fork. Consistent with the above-mentioned assumption that increased fork deceleration favors fork reversal events counteracting fork collapse, less DSBs were oserved in CPT-treated shDEK cells as compared with controls (Figure 2d). This finding might be also explained by the reduced frequency of collisions between replication forks and TOP1-DNA cleavage complexes in slower proliferating shDEK cells.

Figure 4. DEK promotes proliferation upon c-Myc activation. (**a**) Cell cycle analysis of serum-starved NHDF-mycER cells expressing c-MYC and either a nontargeting shRNA (control, -------) or a DEK-specific shRNA (shDEK, - - -) for the indicated time periods. Primary normal human dermal fibroblasts (NHDF) were isolated from human foreskin. Retroviral particles were generated in 293T cells using the pVPack Vectors (Agilent Technologies, Santa Clara, CA, USA) and the pLXSN-mycER retroviral vector. NHDF were infected with retroviral particles and selected with 500 μg/ml G418 and kept as pools. Subsequently, these cells were transduced with lentiviral particles either delivering a scrambled shRNA (control) or a DEK-specific shRNA (shDEK) (pTRIPZ, Open Biosystems, GE Dharmacon, Lafayette, CO, USA) and were selected for 48 h in the presence of 500 μg/ml G418 and 2 μg/ml puromycin. For cell cycle analysis using a LSR Fortessa (BD Bioscences), cells were serum-starved for 48 h, then treated with doxycycline (200 ng/ml, Sigma-Aldrich) or 4-hydroxytamoxifen (1 μM, Sigma-Aldrich) for indicated time periods. Untreated cells served as control. One experiment out of three is shown. Within a histogram, the mean percentage of cells in S phase is shown from three independent experiments (± s.e.m.). Statistical analysis (two-way analysis of variance (ANOVA) with Bonferroni post test) was done using GraphPad Prism 5.02 (GraphPad Software). (**b**) Quantification of the flow cytometry analysis shown in **a**. The Hoechst 33342-specific signal was measured in the gate indicated as 'living cells' to determine mean fluorescence intensities as a measure of mean DNA content. Data represent the mean of three independent cell cycle analyses. Mean intensities are normalized to the value of untreated (0 h) shDEK cells. Error bars represent s.e.m. Statistical analysis (two-way ANOVA with Bonferroni post test) was done using GraphPad Prism 5.02 (GraphPad Software). (**c**) c-MYC-dependent induction of target genes for experiments shown in **a** was verified by quantitative RT PCR (RT qPCR). Cellular mRNA was extracted using the RNeasy Plus Mini Kit (Qiagen, Venlo, Netherland) following the manufacturers' instructions. RT PCR of 1 μg purified mRNA per sample was performed using the reverse transcription system (Promega, Madison, WI, USA). Transcribed mRNA was analyzed by quantitative PCR with SensiMix SYBR Green Mix (Bioline, Luckenwalde, Germany) in a Rotor-Gene Q (Qiagen) machine. Relative mRNA expression was calculated by comparative Ct method and normalized to the housekeeping gene GUS using Rotor-Gene Q software. The following primer pairs were used for amplification: QuantiTect Primer Assays for CYCD2 and ODC (Hs CCND2 1 SG, QT00057575 and Hs ODC1 1 SG, QT00076468; respectively), β-glucuronidase (GUS) forward: 5′-CTCATTTGGAATTTTGCCGATT-3′, β-glucuronidase (GUS) reverse: 5′-CCGAGTGAAGAT-CCCCTTTTTA-3′, DEK forward: 5′-CGAAATGCCCGGTCCCAGAGA-3′, and DEK reverse: 5′-TCGCTTAGCCTTC CTTGCCATTCC-3′. Graphs show the mean of three independent experiments. Statistical analysis (two-way ANOVA with Bonferroni post test) was performed using GraphPad Prism 5.02 (GraphPad Software). Error bars represent s.e.m. (**d**) DNA fiber analysis of NHDF-mycER control and shDEK cells. Cells were either proliferating to measure replication tract lengths under control conditions, or starved and treated with 4-hydroxytamoxifen (4OHT) and doxycycline (DOX) for 4 h to induce c-MYC expression and DEK downregulation as described in **a**. Fiber assay was performed as described in Figure 2a. At least 95 tracts were evaluated per condition. Whiskers indicate 5th 95th percentile. Error bars represent s.e.m. (**e**) DEK downregulation leads to increased long-term accumulation of DNA damage in cells with activated c-MYC expression. Proliferating NHDF-mycER control and shDEK cells were treated with 4-hydroxytamoxifen (4OHT) and doxycycline (DOX) for 9 days. Medium was changed every 2 3 days. Cells were labeled with antibodies specific for γH2AX (anti-phospho H2AX (Ser139), 1:500, clone JBW301, Biomol). Goat anti-mouse Alexa Fluor-488 (Invitrogen) was used as secondary antibodies. Only RFP-positive cells were evaluated (165 cells per condition). γH2AX positive foci were counted using the 'Foci Counter' tool, which is part of the BIC macro toolkit (available online, see legend to Figure 2a). (**f**) Proposed role of DEK in the oncogene-induced DNA replication stress model of tumorigenesis. DEK facilitates proliferation in precancerous cells by promoting replication fork progression and by mitigating the consequences of replication-induced DNA damage. Thereby DEK helps overcoming the DNA damage response barrier to cancer development.

DEK counteracts DNA damage arising from perturbed DNA replication

Delayed completion of DNA replication occurs preferentially at regions with atypical DNA structure such as chromosomal fragile sites. At these sites, the persistence of underreplicated DNA can culminate in the formation of DSBs.[28] As DEK was required for efficient fork progression, we asked whether it would also impact on DNA lesions arising during replication. To this end, we first treated cells with replication inhibitors and analyzed the formation of nuclear foci of DNA repair marker proteins during S phase. Short-term exposure to HU at millimolar concentration leading to replication fork stalling resulted in the induction of 53BP1-positive and γH2AX-positive foci that were much more pronounced in shDEK cells (Supplementary Figures 2A and B). In contrast, no 53BP1 foci were detected after low doses of APH in S phase. APH treatment led to γH2AX foci formation only, which was again more pronounced in shDEK cells (Figures 3a and b). As we did not observe 53BP1-positive foci, and as DSBs are usually identified by the combined occurrence of both γH2AX and 53BP1,[27,29] we conclude that low doses of APH do not induce DSBs in S phase, at least not in our cellular system. We thus speculated that the γH2AX-positive foci observed in APH-treated cells might in part represent unresolved replication intermediates occurring at forks stalled at sites difficult to replicate and containing longer stretches of ssDNA. Indeed, γH2AX was localized at stalled replication forks at early time points preceding the appearance of DSBs by iPOND.[30] Recent work has implicated RAD51, a protein involved in DNA repair by homologous recombination, in the stabilization of stalled forks and protection from MRE11-mediated cleavage of the nascent DNA strand contributing to the restoration of a functional replisome.[31] Therefore we analyzed the formation of RAD51-positive foci in APH-treated cells. Indeed, we observed an increase in RAD51-positive shDEK cells after APH treatment. Interestingly, in these cells γH2AX colocalized partially with RAD51-positive signals and the extent of colocalization was significantly higher in shDEK cells (Figure 3b, right panel) supporting our hypothesis that DEK might help in resolving replication problems at stalled forks. The increase in these double-positive, but 53BP1-negative foci

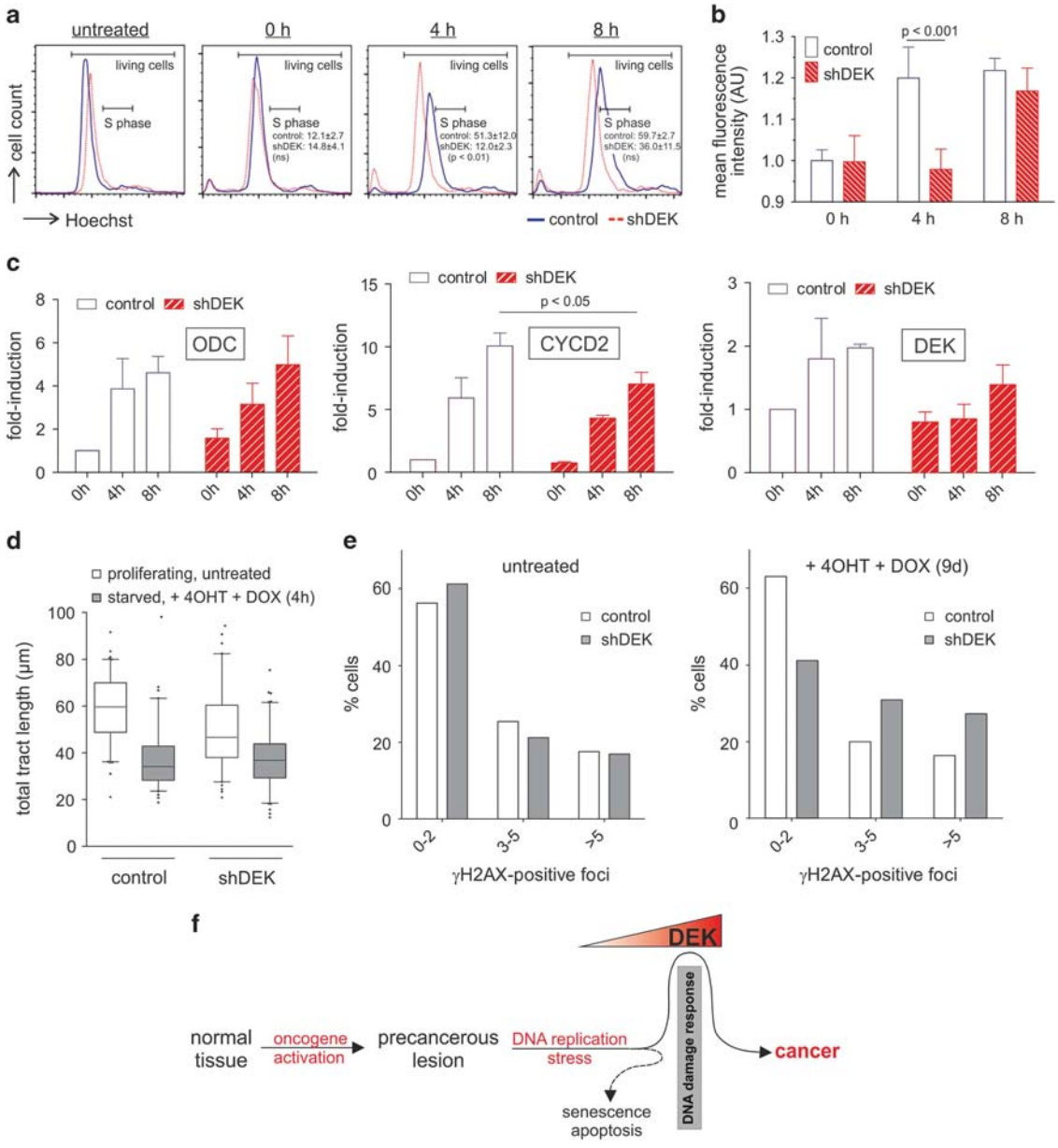

observed in shDEK cells following APH treatment corroborates the notion that DEK might help in solving replication problems and facilitate fork progression under conditions of replication stress.

Recently, a function at the replication fork has been demonstrated also for proteins of the FA (Fanconi anemia) family. They were shown to stabilize collapsed forks in Xenopus cell-free extracts[32] and have been implicated in the protection from replication stress-induced genomic instability.[33] In particular, FANCD2 was shown to be recruited to stalled forks[34] where it contributes to maintain the integrity of single-stranded regions.[35] Interestingly, FANCD2 deficiency can be compensated and functionally rescued by RAD51 overexpression. Thus, these two proteins are epistatic in achieving fork stabilization in replication-inhibited cells.[36] To further analyze the effect of DEK at replication forks, we determined the formation of FANCD2 foci after treatment with APH. Intriguingly, induction of FANCD2-positive foci was much less pronounced in shDEK cells as compared with control cells. These foci did not arise from centromeres, as shown by co-immunostaining with CREST antibodies (Supplementary Figures 3A and B) but most likely represented unresolved replication intermediates as occurring at chromosomal fragile sites, genomic loci that are particularly difficult to replicate and whose rearrangements in tumor cells contribute to cancer development.[33,37] In analogy to chromosomal fragile sites, we detected FANCD2 foci also on anaphase chromosomes after treatment with APH. These foci too, were less abundant in shDEK cells as compared with controls (Supplementary Figures 3C and D). These data establish an interesting link between DEK and the FA pathway. As we did not observe any effect of DEK on FANCD2 protein levels (data not shown), we speculate that DEK might be involved in chromatin remodeling events at stalled or collapsed forks that enable binding of FA proteins and subsequent FANCD2 monoubiquitination. The shDEK-dependent reduction in FANCD2 foci was accompanied by an increased number of RAD51 foci as expected from the above-mentioned compensatory effect.

Taken together, DEK levels impact on replication-born DNA damage in three different models of replication stress and the effects can be interpreted in terms of the different mode of action of replication inhibitors used. In HU-treated cells, DEK downregulation increases the number of DSBs arising from the acute stalling of the replication fork; in APH-treated cells, it increases the number of unresolved replication intermediates forming at decelerated forks; and in CPT-treated cells, it limits DSB formation by a yet unknown mechanism which might involve fork reversals. The molecular events underlying the distinct effects of DEK downregulation on replication inhibition by these drugs will be the subject of future studies.

DEK protects daughter cell generations from replication stress-induced DNA damage

When cells enter mitosis, underreplicated DNA regions arising from impeded replication in S phase are converted to chromosomal breaks by chromatin condensation. The effect of DEK downregulation on the handling of replication problems let us predict that this protein might also limit the level of DNA damage present on mitotic chromosomes. We tested this hypothesis using low-dose APH treatment, which is compatible with continuous replication and leads to the accumulation of underreplicated DNA. In fact, metaphases of shDEK cells treated with APH showed an increased number of γH2AX-positive foci as compared with controls (Figures 3c and d), indicative of the carryover of replicative DNA lesions from S-phase.

To avoid untimely processing and error-prone repair in the subsequent G1 phase, these chromosomal lesions are sequestered in specialized compartments termed 53BP1 nuclear bodies or OPT-domains.[25,38] DEK downregulation significantly augmented the occurrence of 53BP1 nuclear bodies in CYCA-negative G1 phase cells following mild replication stress (Figures 3e and f), in agreement with the results obtained so far. As we have shown recently that recombinant DEK, added directly to the cell culture medium, passes the cell membrane, enters the nucleus and re-engages in its bona fide biological functions, we used this elegant approach for rescue purposes.[11] Indeed, re-added DEK suppressed the formation of 53BP1 nuclear bodies in APH-treated shDEK cells to a level comparable to control cells (Figure 3f). These data evince a role of DEK in safeguarding daughter cells from the consequences of replication-associated DNA damage.

DEK promotes proliferation upon c-MYC activation

Finally we were interested whether DEK might promote proliferation also in the context of oncogene-induced replication stress. To address this question, we used normal human dermal fibroblasts (NHDF) carrying both an inducible *c-MYC* transgene under the control of the estrogen receptor (mycER) and a tetracycline-inducible cassette for expression of either a DEK-specific shRNA (shDEK) or a nontargeting shRNA (control). First, cells were serum-starved to allow for accumulation in G0 phase of the cell cycle (Figure 4a, 0 h). Then, c-MYC upregulation and shRNA expression were induced simultaneously, and cell cycle progression was monitored via flow cytometry. Knockdown of DEK had a negative effect on c-MYC induced proliferation: cells that expressed c-MYC and a nontargeting shRNA began to proliferate within 4 h after c-MYC induction, as demonstrated by increased incorporation of the DNA dye Hoechst 33342 (Figure 4a, 4 h). In contrast, 4 h after c-MYC induction, the DNA content of shDEK cells still corresponded to that of G0 cells (Figure 4b). Eight hours after c-MYC expression, even the shDEK cells had proceeded into S phase. Robust activation of c-MYC target gene expression and DEK downregulation were verified by RT–PCR (Figure 4c). The increase of DEK mRNA in control cells upon c-MYC induction suggests that DEK itself might be a transcriptional target of this oncogene. Eight hours after c-MYC induction, DEK mRNA expression levels increased despite the presence of the DEK-specific shRNA, suggesting that in these cells, c-MYC-dependent DEK upregulation outweighs the effect of RNA interference, and explaining why 8 h after c-MYC induction, the difference in proliferation capacity between shDEK and control cells is diminished.

DNA fiber assays showed a marked reduction of replication fork speed upon oncogene induction (Figure 4d) as compared with proliferating, uninduced cells. Downregulation of DEK did not further exacerbate the effect of oncogene-induced replication fork slowing, differently from treatment with CPT. We interpret this finding as a result of the much more prominent effect of c-MYC on fork progression as compared with CPT, which might conceal a weaker modulatory function of DEK. Finally, we assessed the formation of DNA damage foci in NHDF expressing c-MYC in the presence or absence of DEK (Figure 4e) in a long-term experiment. Nine days after c-MYC induction, we observed an increase in the number of cells with higher number of γH2AX-positive foci as compared with control DEK expressing cells. These data show that DEK promotes proliferation also in the context of oncogene activation possibly via a synergistic effect with oncogene-driven transcription of cell cycle genes. To what extent DEK's modulatory function at the replication fork impacts oncogene-induced fork slowing is not clear yet, and will be the subject of further study. Nonetheless, downregulation of DEK leads to the long-term accumulation of DNA damage in hyperproliferating NHDFs, in support of our hypothesis of DEK acting to counteract replication-born DNA damage.

Taken together, this work provides evidence that the DEK oncoprotein promotes replication fork progression and minimizes the accumulation and transmission of replication stress-induced DNA damage. Both activities can be considered tumor suppressive in an untransformed cell. In cells that have undergone malignant

changes that result in accelerated proliferation, such as oncogene activation, the properties of DEK unveiled by our study may favor genomic restabilization and contribute to overcome the DNA damage barrier of oncogenesis (Figure 4f). Furthermore, extracellular DEK—either actively secreted or released by dying cells[11,12,39]—once taken up by neighboring cells may render them more resistant to replication stress-induced DNA damage and less sensitive towards chemotherapeutic agents interfering with DNA replication thereby negatively influencing tumor prognosis.

CONFLICT OF INTEREST

The authors declare no conflict of interest.

ACKNOWLEDGEMENTS

We thank G Marra for U2 OS cells, Y Marquardt for NHD fibroblasts, J Schmidt for ImageJ Macro programming, D Hermann, K Weidele and F Teusel for technical assistance; S Bürger and the FlowKon facility for support in flow cytometry and M Lopes, C Lukas, A Bürkle and B Lüscher for fruitful discussions. This work was supported by the German Research Foundation (DFG) through funds of the SFB 969, and of the RTG 1331. Work in the laboratory of FK is supported by a DFG grant (KA 2799/1) and by the START program of the Faculty of Medicine, RWTH Aachen.

REFERENCES

1 Kappes F, Waldmann T, Mathew V, Yu J, Zhang L, Khodadoust MS *et al.* The DEK oncoprotein is a Su(var) that is essential to heterochromatin integrity. *Genes Dev* 2011; **25**: 673 678.
2 Waldmann T, Eckerich C, Baack M, Gruss C. The ubiquitous chromatin protein DEK alters the structure of DNA by introducing positive supercoils. *J Biol Chem* 2002; **277**: 24988 24994.
3 Cheung TH, Quach NL, Charville GW, Liu L, Park L, Edalati A *et al.* Maintenance of muscle stem cell quiescence by microRNA 489. *Nature* 2012; **482**: 524 528.
4 Wise Draper TM, Morreale RJ, Morris TA, Mintz Cole RA, Hoskins EE, Balsitis SJ *et al.* DEK proto oncogene expression interferes with the normal epithelial differentiation program. *Am J Pathol* 2009; **174**: 71 81.
5 Wise Draper TM, Allen HV, Thobe MN, Jones EE, Habash KB, Münger K *et al.* The human DEK proto oncogene is a senescence inhibitor and an upregulated target of high risk human papillomavirus E7. *J Virol* 2005; **79**: 14309 14317.
6 Wise Draper TM, Allen HV, Jones EE, Habash KB, Matsuo H, Wells SI. Apoptosis inhibition by the human DEK oncoprotein involves interference with p53 functions. *Mol Cell Biol* 2006; **26**: 7506 7519.
7 von Lindern M, Fornerod M, van Baal S, Jaegle M, de Wit T, Buijs A *et al.* The translocation (6;9), associated with a specific subtype of acute myeloid leukemia, results in the fusion of two genes, dek and can, and the expression of a chimeric, leukemia specific dek can mRNA. *Mol Cell Biol* 1992; **12**: 1687 1697.
8 Kappes F, Khodadoust MS, Yu L, Kim DS, Fullen DR, Markovitz DM *et al.* DEK expression in melanocytic lesions. *Hum Pathol* 2011; **42**: 932 938.
9 Khodadoust MS, Verhaegen M, Kappes F, Riveiro Falkenbach E, Cigudosa JC, Kim DSL *et al.* Melanoma proliferation and chemoresistance controlled by the DEK oncogene. *Cancer Res* 2009; **69**: 6405 6413.
10 Wise Draper TM, Mintz Cole RA, Morris TA, Simpson DS, Wikenheiser Brokamp KA, Currier MA *et al.* Overexpression of the cellular DEK protein promotes epithelial transformation *in vitro* and *in vivo*. *Cancer Res* 2009; **69**: 1792 1799.
11 Saha AK, Kappes F, Mundade A, Deutzmann A, Rosmarin DM, Legendre M *et al.* Intercellular trafficking of the nuclear oncoprotein DEK. *Proc Natl Acad Sci USA* 2013; **110**: 6847 6852.
12 Kappes F, Fahrer J, Khodadoust MS, Tabbert A, Strasser C, Mor Vaknin N *et al.* DEK is a poly(ADP ribose) acceptor in apoptosis and mediates resistance to genotoxic stress. *Mol Cell Biol* 2008; **28**: 3245 3257.
13 Kavanaugh GM, Wise Draper TM, Morreale RJ, Morrison MA, Gole B, Schwemberger S *et al.* The human DEK oncogene regulates DNA damage response signaling and repair. *Nucleic Acids Res* 2011; **39**: 7465 7476.
14 Fahrer J, Popp O, Malanga M, Beneke S, Markovitz DM, Ferrando May E *et al.* High affinity interaction of poly(ADP ribose) and the human DEK oncoprotein depends upon chain length. *Biochemistry* 2010; **49**: 7119 7130.
15 Hanahan D, Weinberg RA. Hallmarks of cancer: the next generation. *Cell* 2011; **144**: 646 674.
16 Alexiadis V, Waldmann T, Andersen J, Mann M, Knippers R, Gruss C. The protein encoded by the proto oncogene DEK changes the topology of chromatin and reduces the efficiency of DNA replication in a chromatin specific manner. *Genes Dev* 2000; **14**: 1308 1312.
17 Waldmann T, Baack M, Richter N, Gruss C. Structure specific binding of the proto oncogene protein DEK to DNA. *Nucleic Acids Res* 2003; **31**: 7003 7010.
18 Riveiro Falkenbach E, Soengas MS. Control of tumorigenesis and chemoresistance by the DEK oncogene. *Clin Cancer Res* 2010; **16**: 2932 2938.
19 Bartkova J, Horejsi Z, Koed K, Kramer A, Tort F, Zieger K *et al.* DNA damage response as a candidate anti cancer barrier in early human tumorigenesis. *Nature* 2005; **434**: 864 870.
20 Halazonetis TD, Gorgoulis VG, Bartek J. An oncogene induced DNA damage model for cancer development. *Science* 2008; **319**: 1352 1355.
21 Bartek J, Mistrik M, Bartkova J. Thresholds of replication stress signaling in cancer development and treatment. *Nat Struct Mol Biol* 2012; **19**: 5 7.
22 Murga M, Campaner S, Lopez Contreras AJ, Toledo LI, Soria R, Montana MF *et al.* Exploiting oncogene induced replicative stress for the selective killing of Myc driven tumors. *Nat Struct Mol Biol* 2011; **18**: 1331 1335.
23 Petermann E, Orta ML, Issaeva N, Schultz N, Helleday T. Hydroxyurea stalled replication forks become progressively inactivated and require two different RAD51 mediated pathways for restart and repair. *Mol Cell* 2010; **37**: 492 502.
24 Trenz K, Smith E, Smith S, Costanzo V. ATM and ATR promote Mre11 dependent restart of collapsed replication forks and prevent accumulation of DNA breaks. *EMBO J* 2006; **25**: 1764 1774.
25 Lukas C, Savic V, Bekker Jensen S, Doil C, Neumann B, Pedersen RS *et al.* 53BP1 nuclear bodies form around DNA lesions generated by mitotic transmission of chromosomes under replication stress. *Nat Cell Biol* 2011; **13**: 243 253.
26 Wilhelm T, Magdalou I, Barascu A, Techer H, Debatisse M, Lopez BS. Spontaneous slow replication fork progression elicits mitosis alterations in homologous recom bination deficient mammalian cells. *Proc Natl Acad Sci USA* 2014; **111**: 763 768.
27 Ray Chaudhuri A, Hashimoto Y, Herrador R, Neelsen KJ, Fachinetti D, Bermejo R *et al.* Topoisomerase I poisoning results in PARP mediated replication fork reversal. *Nat Struct Mol Biol* 2012; **19**: 417 423.
28 Debatisse M, Le Tallec B, Letessier A, Dutrillaux B, Brison O. Common fragile sites: mechanisms of instability revisited. *Trends Genet* 2012; **28**: 22 32.
29 de Feraudy S, Revet I, Bezrookove V, Feeney L, Cleaver JE. A minority of foci or pan nuclear apoptotic staining of gammaH2AX in the S phase after UV damage contain DNA double strand breaks. *Proc Natl Acad Sci USA* 2010; **107**: 6870 6875.
30 Sirbu BM, McDonald WH, Dungrawala H, Badu Nkansah A, Kavanaugh GM, Chen Y *et al.* Identification of proteins at active, stalled, and collapsed replication forks using isolation of proteins on nascent DNA (iPOND) coupled with mass spectrometry. *J Biol Chem* 2013; **288**: 31458 31467.
31 Hashimoto Y, Ray Chaudhuri A, Lopes M, Costanzo V. Rad51 protects nascent DNA from Mre11 dependent degradation and promotes continuous DNA synthesis. *Nat Struct Mol Biol* 2010; **17**: 1305 1311.
32 Wang LC, Stone S, Hoatlin ME, Gautier J. Fanconi anemia proteins stabilize replication forks. *DNA Repair (Amst)* 2008; **7**: 1973 1981.
33 Naim V, Rosselli F. The FANC pathway and BLM collaborate during mitosis to prevent micro nucleation and chromosome abnormalities. *Nat Cell Biol* 2009; **11**: 761 768.
34 Bogliolo M, Lyakhovich A, Callén E, Castellà M, Cappelli E, Ramírez MJ *et al.* Histone H2AX and Fanconi anemia FANCD2 function in the same pathway to maintain chromosome stability. *EMBO J* 2007; **26**: 1340 1351.
35 Renaud E, Rosselli F. FANC pathway promotes UV induced stalled replication forks recovery by acting both upstream and downstream Poleta and Rev1. *PLoS ONE* 2013; **8**: e53693.
36 Schlacher K, Wu H, Jasin M. A distinct replication fork protection pathway connects Fanconi anemia tumor suppressors to RAD51 BRCA1/2. *Cancer Cell* 2012; **22**: 106 116.
37 Chan KL, Palmai Pallag T, Ying S, Hickson ID. Replication stress induces sister chromatid bridging at fragile site loci in mitosis. *Nat Cell Biol* 2009; **11**: 753 760.
38 Harrigan JA, Belotserkovskaya R, Coates J, Dimitrova DS, Polo SE, Bradshaw CR *et al.* Replication stress induces 53BP1 containing OPT domains in G1 cells. *J Cell Biol* 2011; **193**: 97 108.
39 Mor Vaknin N, Punturieri A, Sitwala K, Faulkner N, Legendre M, Khodadoust MS *et al.* The DEK nuclear autoantigen is a secreted chemotactic factor. *Mol Cell Biol* 2006; **26**: 9484 9496.